DTU Library

Imaging blood's velocity using synthetic aperture ultrasound

Jensen, Jørgen Arendt; Li, Ye

Published in:
9th European Conference on synthetic Aperture Radar

Publication date:
2012

Document Version
Peer reviewed version

Imaging blood's velocity using synthetic aperture ultrasound

Jørgen Arendt Jensen and Ye Li
Center for Fast Ultrasound Imaging, Dept. of Elec. Eng. Bldg. 349,
Technical University of Denmark, DK-2800 Lyngby, Denmark

Abstract

The blood velocity vector can be estimated using synthetic aperture techniques in medical ultrasound by using short emission sequences. The whole image region is insonified and the flow can be tracked in all directions continuously. This is a major advantage compared to commercial systems, since the separation between blood and tissue is greatly eased by this, and the estimates can be averaged over long time than in traditional systems. Vector velocity imaging can, thus, be made and attain an order of magnitude higher precision than in current commercial systems and at higher frame rates. It is also possible to visualize very slow moving flow. The paper will present methods for making such imaging.

1 Velocity estimation in medical ultrasound

The blood velocity be estimated in medical ultrasound and displayed as the color flow map image shown in Fig. 1. Here a blue color indicates velocity towards the transducer and red away from the transducer. The velocity is estimated by acquiring 8 to 16 focused ultrasound lines in the same direction. The velocity is estimated from either the phase shift between consecutive lines [8, 12] or the time shift estimation [1, 2, 4].

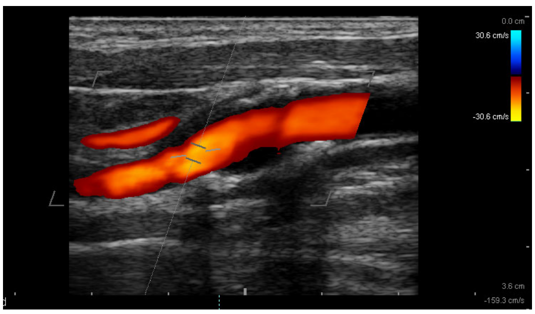

Figure 1: Conventional color flow map image of the internal carotid artery.

The time shift is generated by the motion between pulse emissions, which along the ultrasound beam is

$$\Delta z = T_{prf} v_z = T_{prf} |v| \cos\theta.$$

Here T_{prf} is the time between plus emissions, v_z is the axial velocity, $|v|$ is the velocity magnitude and θ is the angle between the ultrasound beam and the flow direction. Δz is translated to a time shift as

$$t_s = \frac{2|v|\cos\theta}{c} T_{prf} = \frac{2\Delta z}{c} T_{prf}$$

where c is the speed of sound. The velocity is then found by cross-correlating two consequitive measurements $y_1(t)$ and $y_2(t) = y_1(t - t_s)$:

$$\begin{aligned} R_{12}(\tau) &= \int y_1(t) y_2(t+\tau) dt \\ &= \int y_1(t) y_1(t - t_s + \tau) dt = R_{11}(\tau - t_s), \end{aligned} \tag{1}$$

where $R_{11}(\tau)$ is the autocorrelation of the received signal. The position of the maximum value in $R_{12}(\tau)$ is, thus, directly related to the axial velocity.

The currently used methods have two major limitations: only the axial velocity component can be detected due to the $\cos\theta$ factor and the estimates often have a high variance due to the few samples acquired in each direction. This is difficult to increase as the frame rate then drops and makes the images less useful for studying the pulsating flow in the human body. Methods that can find the velocity vector and at the same time increase the information acquisition rate is therefore of great interest.

2 Synthetic aperture velocity estimation

One possible solution to the problems is to use synthetic aperture imaging for acquiring the data. The sequential line acquisition in one direction at a time in conventional ultrasound is replaced by insonifying the whole image region. A spherical wave is emitted from one or a couple of elements and insonifies the whole region. The scattered field is then received by all transducer elements. The process is repeated for all transmitting elements on the aperture and for each emission a low resolution image (LRI) is formed by focusing the received data. All the low resolution images are then added and this ensures that a dynamic transmit focusing is attained [6, 13]. The resulting images, thus, have dynamic focusing during in both transmit and receive, and a higher image quality is attained. The imaging can also be made fast by only employing few transmit events for each high resolution image at the expense of higher side-lobes in the resulting point spread function.

Such an imaging scheme can also be used for flow estimation. The complication here is that the object moves during the acquisition and the data are, thus, not fully in phase. This will only slightly distort the data as the motion is small for the pulse emission times in medical ultrasound. The speed of sound is 1540 m/s in human tissue and imaging down to 15 cm takes 200 μs giving a pulse repetition frequency of 5 kHz. Typically peak blood velocities are around 1 m/s giving a maximum motion of 0.2 mm between emissions. The point spread function is affected by this, and it is important to take this change into account. This is done by using short emission sequences as shown in Fig. 2, where a sequence with 2 emissions are repeated. Each column in the graph shows the emitting aperture, the resulting point spread function (PSF) for the LRI, the addition of LRIs, and finally the high resolution image (HRI) as the shaded gray PSF in the bottom.

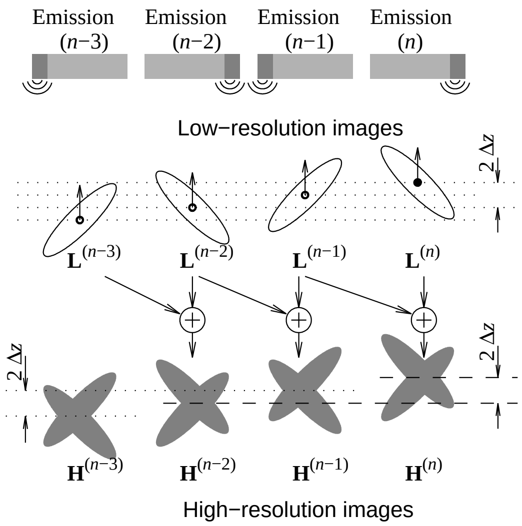

Figure 2: Principle of synthetic aperture velocity imaging (from [14]).

The point scatterer is moving towards the transducer, and the PSF is different for the combination of emission 1 and 2 from the combination of 2 and 3, and this severely affects the correlation between the two signals. However, the PSF for the combination of emissions 1 and 2 and the PSF from emissions 3 and 4 are similar, apart from the translation towards the transducer. The motion can therefore be found by correlating these two PSFs and the shift in position can be found [14]. Dividing by the time between the two PSFs directly gives the axial velocity.

The approach has several advantages. Foremost the whole region is insonified continuously. Therefore data can be beamformed everywhere in the region continuously and the moving blood can be tracked continuously. The beamformed data can, thus, be correlated over as much time as the velocity is quasi-stationary, and this significantly increase the accuracy of the velocity estimates. A second advantage is that data can be beamformed in any direction, and this can be used for solving the angle problem. The true velocity magnitude can be found by beamforming focused lines along the flow direction as shown in Fig. 3. Cross-correlating these lines then directly can reveal the motion in the direction and dividing by the time directly gives the velocity magnitude [7].

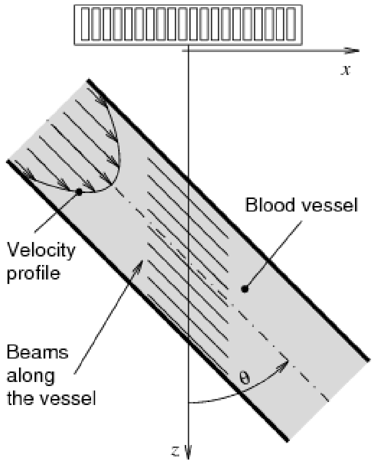

Figure 3: Directional beamforming (from [7]).

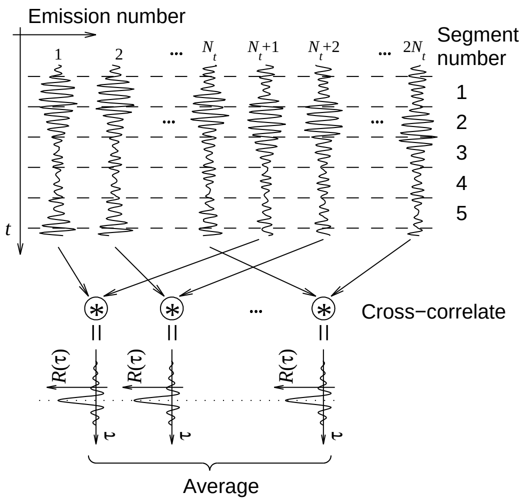

Figure 4: Averaging of the cross-correlation function for the different emissions (from [7]).

The cross-correlation of the data is shown in Fig. 4. Here data from the same emission sequence is cross-correlated, so data from emission n and $n + N_t$ are correlated, where

N_t is the period of the emission sequence. These cross-correlation functions are then averaged over the time the flow can be considered quasi-stationary to optimize the estimate.

SA imaging and directional beamforming can significantly increase the accuracy of velocity estimation. An example is shown in Fig. 5 for a flow perpendicular to the ultrasound beam, where a traditional system would not be able to detect the it. For the SA acquisition 8 emission spaced over the aperture were used and this was repeated 16 times. The velocity was then detected by cross-correlating the lines. A standard deviation of 1.2% was attained [7], which is an order of magnitude more precise than current systems, so this give a fully quantitative estimate. Also the imaging is fairly fast. 128 emissions are used for one image and using a pulse repetition frequency of 5 kHz gives roughly 40 images a second that can cover the full heart. A conventional color flow image would require around 4-500 emissions to cover the same region.

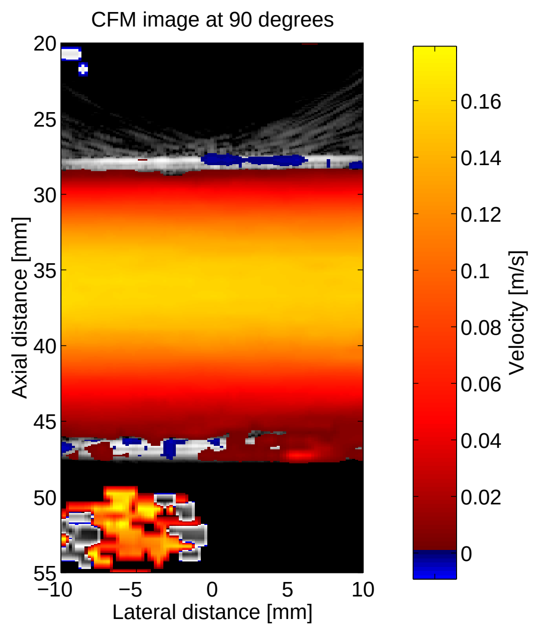

Figure 5: Directional velocity image at 90 degrees (from [7]).

3 Dual stage flow imaging

The major disadvantage SA flow imaging is the huge number of calculations to be performed per second. A full image along the flow directions have to be beamformed for each pulse emission, which often is at least 100 - 1000 times more than for a conventional scanner. This currently precludes a real time implementation of the approach on commercial platforms and other more efficient approaches must be developed.

A possible solution is to employ dual stage beam forming, which divides the processing into two steps [9]. A first stage that consist of a simple static beamformer with a fixed focus in both transmit and receive as shown in Fig. 6. This reduces the data from the multiple elements in receive to a single signal that is then used in the next stage beamformer. Here the signals from all the first stage beamformers are combined to a dynamically focused signal as illustrated in Fig. 6. The green dots indicate three different image point and how the data are combined from the first stage signals. This approach reduces the number of calculations by the number of receiving elements and the amount of data correspondingly and, thus, makes it possible to implement. The approach maintains the advantages of synthetic aperture imaging with a slight reduction is image quality, but it is still an improvement compared to traditional imaging [3].

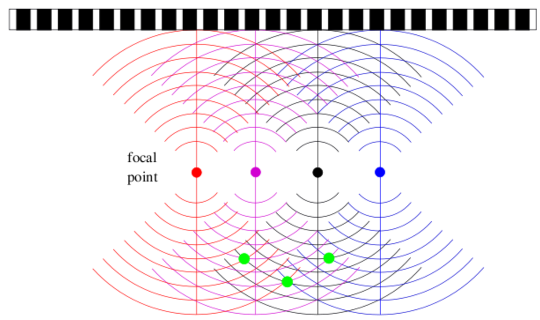

Figure 6: Dual stage beamforming approach.

The method can also be applied to flow imaging. Here a short sequence of emissions are repeated continuously. The received first stage data is then beamformed in short focused lines that are oriented along the flow direction and positioned symmetrically around the point where the velocity should be found [10, 11]. Such an approach has been used in Fig. 7

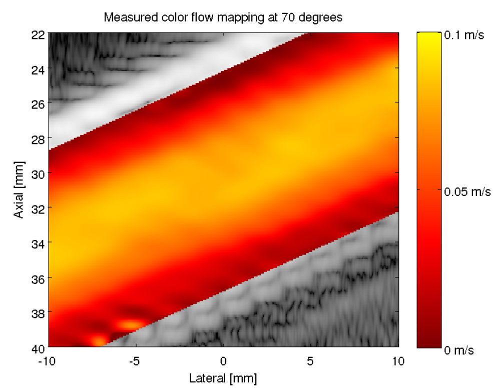

Figure 7: Dual stage velocity image at 70 degrees (from [11]).

In this example four emissions are used spaced 7λ apart, and the first stage beamformer is focused 5 mm from the surface. 64 elements are used in transmit and receive, and the emission sequence is repeated 12 times, so the full image is generated in 48 emissions. The transmission and reception is made by the experimental ultrasound scanner SARUS [5] and all the channel data is sampled and stored on disk for off-line processing. The flow is generated by a circulating flow rig system generating a parabolic flow with a with a peak velocity of 0.1 m/s. The angle between the flow and the and ultrasound propagation direction is 70 degrees. In this example the relative standard deviation and bias are 4.3% and 4.2%, respectively [11].

4 Conclusion

Synthetic aperture imaging can be adapted for flow estimation. This is done by using short, repeated emission sequences and then correlate data obtained with similar scan sequences. The approach has several advantages compared to traditional velocity estimation. Foremost the full region is interrogated continuously and this makes it possible to track the motion continuously. For these system it is, thus, much easier to separate stationary tissue and flowing blood as the estimates can be averaged over considerably longer time making it possible to detect very slow moving flow. The imaging can also be made fast as the number of emissions for a full image often can be limited to 50-100. This translates into a frame rate of 50-100 Hz even for larger structures as the heart. The introduction of dual stage beam forming also makes it possible to reduce the number of calculations dramatically and paves the way for possible commercial implementations.

Acknowledgement

This work was supported by grant 9700883, 9700563 and 26-04-0024 from the Danish Science Foundation and by B-K Medical Aps. This project is also supported by grant 024-2008-3 from the Danish Advanced Technology Foundation

References

[1] O. Bonnefous and P. Pesqué. Time domain formulation of pulse-Doppler ultrasound and blood velocity estimation by cross correlation. *Ultrason. Imaging*, 8:73–85, 1986.

[2] S. G. Foster, P. M. Embree, and W. D. O'Brien. Flow velocity profile via time-domain correlation: Error analysis and computer simulation. *IEEE Trans. Ultrason., Ferroelec., Freq. Contr.*, 37:164–175, 1990.

[3] M. C. Hemmsen, P. M. Hansen, T. Lange, J. M. Hansen, M. B. Nielsen, , and J. A. Jensen. Preliminary In-Vivo evaluation of Synthetic Aperture Sequential Beamformation using a multielement convex array. In *Proc. IEEE Ultrason. Symp.*, page Accepted, Oct. 2011.

[4] J. A. Jensen. *Estimation of Blood Velocities Using Ultrasound: A Signal Processing Approach*. Cambridge University Press, New York, 1996.

[5] J. A. Jensen, H. Holten-Lund, R. T. Nielson, B. G. Tomov, M. B. Stuart, S. I. Nikolov, M. Hansen, and U. D. Larsen. Performance of SARUS: A Synthetic Aperture Real-time Ultrasound System. In *Proc. IEEE Ultrason. Symp.*, pages 305–309, Oct. 2010.

[6] J. A. Jensen, S. Nikolov, K. Løkke Gammelmark, and M. Høgholm Pedersen. Synthetic aperture ultrasound imaging. *Ultrasonics*, 44:e5–e15, 2006.

[7] J. A. Jensen and S. I. Nikolov. Directional synthetic aperture flow imaging. *IEEE Trans. Ultrason., Ferroelec., Freq. Contr.*, 51:1107–1118, 2004.

[8] C. Kasai, K. Namekawa, A. Koyano, and R. Omoto. Real-Time Two-Dimensional Blood Flow Imaging using an Autocorrelation Technique. *IEEE Trans. Son. Ultrason.*, 32:458–463, 1985.

[9] J. Kortbek, J. A. Jensen, and K. L. Gammelmark. Synthetic aperture sequential beamforming. In *Proc. IEEE Ultrason. Symp.*, pages 966–969, 2008.

[10] Y. Li and J. A. Jensen. Synthetic aperture flow imaging using a dual stage beamformer approach. In *Proc. IEEE Ultrason. Symp.*, pages 1924–1927, 2010.

[11] Y. Li and J. A. Jensen. Directional synthetic aperture flow imaging using a dual stage beamformer approach. In *Proc. IEEE Ultrason. Symp.*, page Accepted, 2011.

[12] T. Loupas, J. T. Powers, and R. W. Gill. An axial velocity estimator for ultrasound blood flow imaging, based on a full evaluation of the Doppler equation by means of a two-dimensional autocorrelation approach. *IEEE Trans. Ultrason., Ferroelec., Freq. Contr.*, 42:672–688, 1995.

[13] S. I. Nikolov. *Synthetic Aperture Tissue and Flow Ultrasound Imaging*. PhD thesis, Ørsted•DTU, Technical University of Denmark, 2800, Lyngby, Denmark, 2001.

[14] S. I. Nikolov and J. A. Jensen. In-vivo Synthetic Aperture Flow Imaging in Medical Ultrasound. *IEEE Trans. Ultrason., Ferroelec., Freq. Contr.*, 50(7):848–856, 2003.